THERMAL STRESS AND FAILURE LOCATION ANALYSIS FOR THROUGH SILICON VIA IN 3D INTEGRATION

H.-Y. Tsai* **C.-W. Kuo**

Department of Power Mechanical Engineering
National Tsing Hua University
Hsinchu, Taiwan

ABSTRACT

Through silicon via (TSV) is the critical structure for three dimensional (3D) integration, which provides vertical interconnection between stacking dies. In TSV structure, large coefficient differences of thermal expansion exist between silicon substrate, dielectric material, and filled metal. Due to the large thermal mismatch, the high thermal stress occurring at the interface of different materials would result in delamination. Therefore, thermal-mechanical reliability is a key issue for 3D integration. In this study, we investigated the thermal-mechanical stress distribution of TSV under the condition of the accelerated thermal cycling loading by finite element analysis based on a 3D model of TSV structure. Due to the thermal expansion, that the TSV structure squeezed the surface area between TSVs at a high temperature resulted in compressive stresses at the surface area between TSVs. Therefore, a proper distance between the stress-sensitive device and the TSV should be kept. The stress analysis shows that the maximum thermal stress occurs in the outside region of TSV interface and in the annular region of TSV at a high temperature and at a low temperature, respectively. This study helps to obtain a clear thermal stress distribution of TSV and possible failure regions can be determined.

Keywords: Failure location analysis, Through silicon via, Thermal stress, 3D integration.

1. INTRODUCTION

Over the few years, integrated circuits (ICs) have been enhanced primarily by continuously scaling down the size of transistors. However, scaling down of semiconductor device encounters the physical limit; therefore, making ICs into three dimensional structures instead of traditional two dimensional ones is proposed. Recently, a lot of three-dimensional (3D) chip integration research has been done for the next possible revolution of electronic chip device. 3D chip integration has many advantages over traditional IC such as higher IC density, integration of heterogeneous device, and lower power consumption [1]. Through silicon via (TSV) is the critical structure for 3D integration which provides vertical interconnection between stacking dies. However, there are still some challenges for this technology. In TSV structure, there are large coefficient differences of thermal expansion (CTE) between silicon substrate, dielectric material, and filled metal. For example, the CTE of copper is six times larger than that of silicon dioxide. Due to the large thermal mismatch, the high thermal stress at the interface of different materials would result in materials failure or delamination [2-8] and reduce the life of electronic device. Therefore, the thermal-mechanical reliability of TSV structure is a key issue for the development of three-dimensional integration technology. A great amount of research has been done on the study of the thermal stress state and reliability in TSV through finite element modeling technique [7,8]. Some focused on the impact of thermal stress for different dimensional parameters of TSV [4,8-10]. Some investigated the crack growth and delamination in the TSV structure [10-12]. Optimizing parametric design was made by Ladani [13] and Che *et al.* [14]. Dudek *et al.* focused on the induced stress during the TSV manufacturing process [15]. Judging from these results, we know that the thermal stress mainly increases with the via diameter and the CTE of filled material.

In this study, we investigated the thermal-mechanical stress distribution of a 2 × 2 TSV array under the condition of the accelerated thermal cycling loading through finite element analysis (FEA) software-ANSYS®. To get more realistic and more accurate result, a detailed three-dimensional model of TSV structure rather than a two-dimensional one is proposed.

2. THERMAL-MECHANICAL FEA MODEL DESCRIPTION

In this study, three dimensional axis-symmetric models are used to investigate the thermal stress distribution in 2 × 2 annular TSV array. The assumptions in these models are as follows:

1. All material properties used in FEA are assumed to

* Corresponding author (hytsai@pme.nthu.edu.tw)

DOI : 10.1017/jmech.2015.52
Copyright © 2015 The Society of Theoretical and Applied Mechanics, R.O.C.
https://doi.org/10.1017/jmech.2015.52 Published online by Cambridge University Press

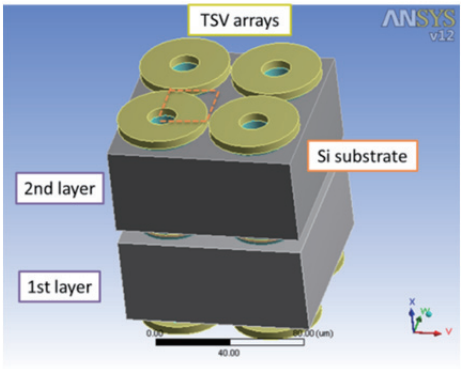
be isotropic and temperature independent.

2. The stress free temperature in these models are set at 25°C.
3. In this model, the interfaces of different materials remain connectedly during the temperature cycling. The voids and cracks at the interface are ignored.

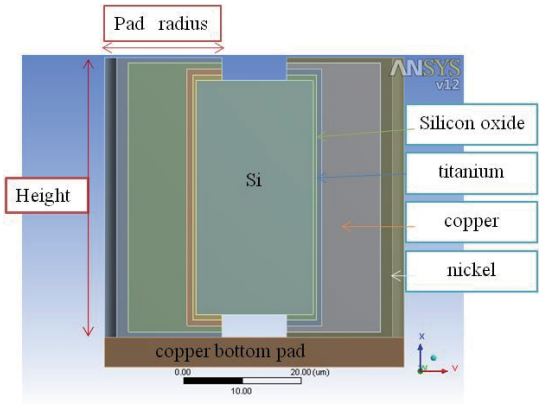
The schematic diagram, cross-section and material properties of the TSV structures in this study are shown in Fig. 1 and Table 1, respectively. Besides, in order to simulate the plastic deformation of metals, we apply plastic material properties to copper and nickel as shown in Table 2.

Table 1 Material properties.

Material	Young's modulus (GPa)	Yield strength (MPa)	Ultimate strength (MPa)	Poisson ratio	CTE (ppm/°C)
Copper	128	150	350	0.36	17
Nickel	200	300	500	0.31	13.1
Silicon	165	–	7000	0.22	3.26
Silicon Dioxide	70	–	110	0.17	0.4
Titanium	110	140	220	0.34	8.9
Tungsten	400	750	980	0.28	4.4



(a) Schematic diagram of the TSV



(b) Cross-section and material of TSV structure

Fig. 1 (a) Schematic diagram of the TSV, (b) Cross-section and material of TSV structure.

Figure 2 shows the boundary conditions in the current model. The boundary conditions in TSV structure are a fixed support underneath the copper bottom pads to simulate the TSV structure assemblies on the pad. The temperature is loaded for all bodies in these models to simulate the thermal loading condition of the accelerated thermal cycling reliability from JDEC accelaterted temperature cycling standard — from –40 °C to 125 °C. Symmetry boundary conditions are applied on all the faces to make the model a 1/4 one to reduce the computational time.

3. RESULT AND DISCUSSION

3.1 Thermal Stress Distribution of TSV Array

Figure 3 shows the von Mises stress distribution when the temperature ramps up from stress free at the temperature of 25°C to 125°C. The maximum von Mises stress (300MPa) of the TSV structure occurs on the nickel surface and on the silicon surface as shown in Fig. 3. The yield strength of nickel is 59MPa and the ultimate tensile strength is 317MPa [16], so it reveals that the stress may result in the break of the nickel from the annular edge of TSV. Figure 4 is the max principal stress distribution for TSV array model when the temperature ramps up from 25°C to 125°C. The maximum principal stress on the silicon surface is about tensile stress of 230MPa and the bottom pad surface area is stretched by the copper pad. These result in tensile stress on the interface of silicon and silicon dioxide. The stress is high enough to result in the break of the silicon from the TSV and silicon edge.

Figure 5 is the von Mises stress distribution when the temperature ramps down from stress free at the temperature of 25°C to –40°C. The maximum von Mises stress of the TSV structure is 300 MPa on nickel surface, so it reveals that the stress may result in the break of the nickel from the annular edge of TSV. Figure 6 shows

Table 2 Plastic Material Properties.

Material	Yield strength (MPa)	Tangent Modulus (MPa)
Copper	150	650
Nickel	300	445

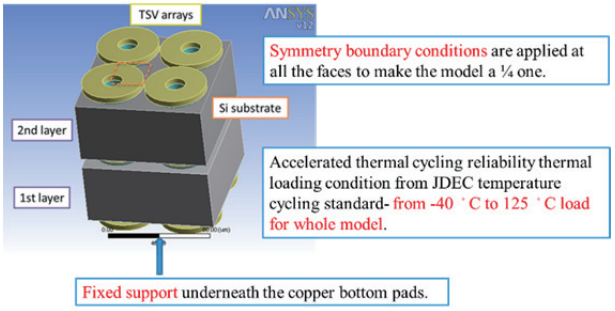


Fig. 2 Boundary conditions.

https://doi.org/10.1017/jmech.2015.52 Published online by Cambridge University Press

the maximum principal stress distribution for TSV array model when the temperature ramps down from 25°C to –40°C. The maximum principal stress on the nickel surface is about tensile stress of 339MPa. That the annular nickel surface area is stretched by the copper results in the tensile stress on the annular nickel surface. This may also result in the delamination of the nickel from this area.

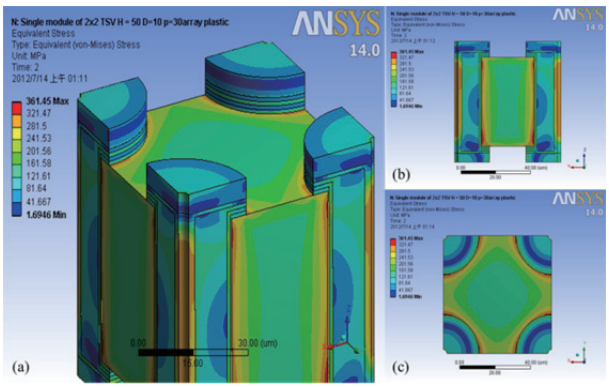


Fig. 3 von Mises stress distribution for TSV array model when the temperature ramps up from 25°C to 125°C: (a) whole mode; (b) side view; (c) bottom view.

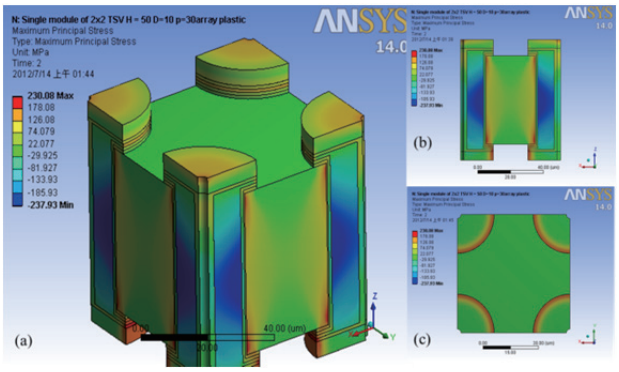


Fig. 4 Maximum principal stress distribution for TSV array model when the temperature ramps up from 25°C to 125°C: (a) whole model; (b) side view; (c) bottom view.

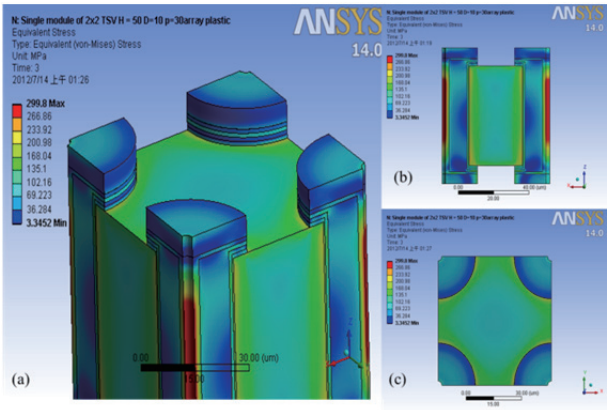


Fig. 5 von Mises stress distribution for TSV array model when the temperature ramps down from 25°C to –40°C: (a) whole mode; (b) side view; (c) bottom view.

3.2 Thermal Stress Distribution of TSV Bonding

In this section, two layers of TSV are bonded to simulate the thermal stress distribution of TSV bonding area under the condition of the accelaterted temperature cycling. Figure 7 shows the von Mises stress distribution for TSV bonding model when the temperature ramps up from 25°C to 125°C. The stress concentration occurs at the silicon area near the bonding pad. Figure 8 shows the maximum principal stress distribution for TSV bonding model when the temperature ramps up from 25°C to 125°C. It reveals that the nickel is stretched by the copper and the tensile stress occurs at the bonding edge.

Figures 9 and 10 show the von Mises stress distribution and the maximum principal stress distributions for TSV bonding model when the temperature ramps down from 25°C to –40°C, respectively. The tensile stress occurs on the nickel annular edge and failure may occur on the annular edge.

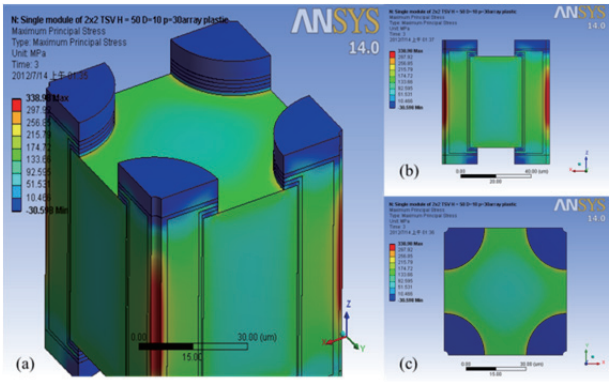


Fig. 6 Maximum principal stress distribution for TSV array model when the temperature ramps down from 25°C to –40°C: (a) whole model; (b) side view; (c) bottom view.

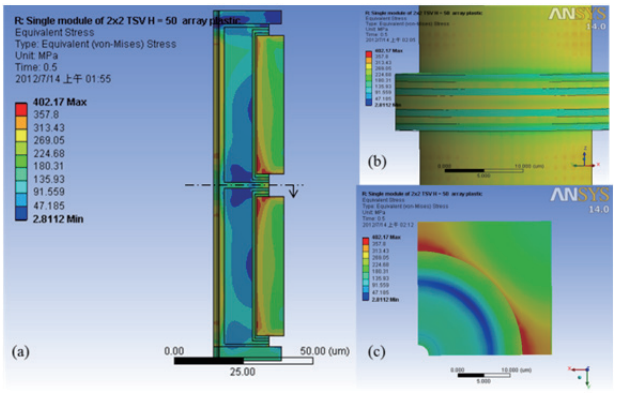


Fig. 7 von Mises stress distribution for TSV bonding model when the temperature ramps up from 25°C to 125°C: (a) whole mode; (b) side view; (c) bottom view.

https://doi.org/10.1017/jmech.2015.52 Published online by Cambridge University Press

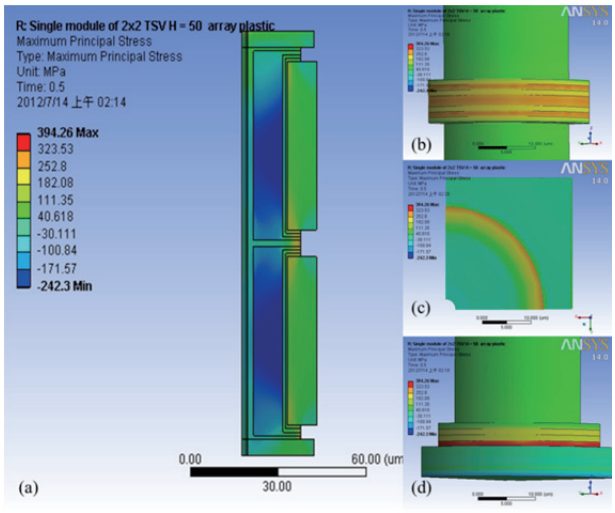


Fig. 8 Maximum principal stress distribution for TSV bonding model when the temperature ramps up from 25°C to 125°C: (a) whole mode; (b) side view; (c) bottom view; (d) bottom pad side view.

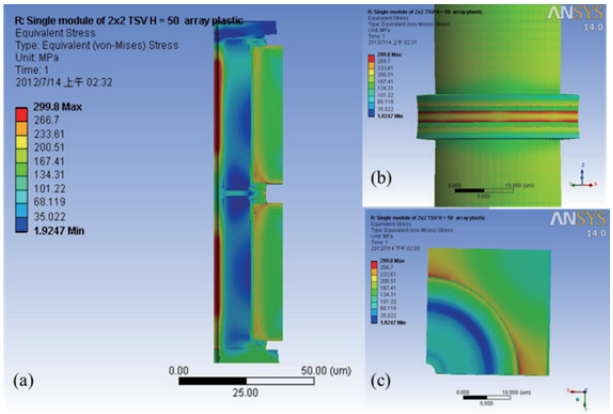


Fig. 9 von Mises stress distribution for TSV bond model when the temperature ramps down from 25°C to –40°C: (a) whole mode; (b) side view; (c) bottom view.

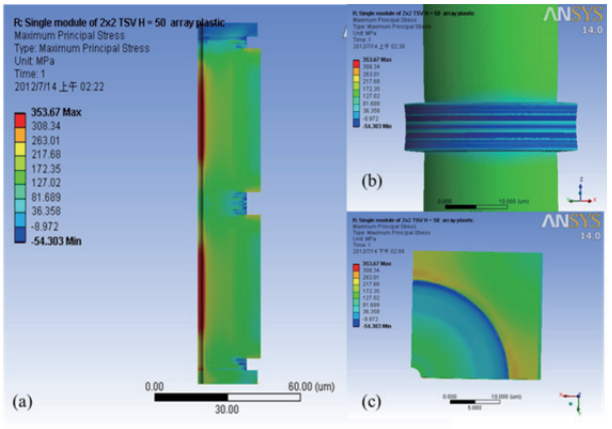


Fig. 10 Maximum principal stress distribution for TSV bond model when the temperature ramps down from 25°C to –40°C: (a) whole model; (b) side view; (c) bottom view.

3.3 Diameter Ratio Study

In this section, we change some geometric parameters of TSV to explore the effect of different geometric parameters and the maximum on Mises stress when the temperature ramps up from 25°C to 125°C. For the annular TSV, we define the diameter ratio which represents the annular effect in TSV, as below

$$\text{Diameter Ratio} = (D_o - D_i)/D_o$$

where D_o and D_i are the outside and inside diameters of TSV, respectively.

As shown in Fig. 11, the simulation result reveals that the maximum von Mises stress at 125°C increases with the diameter ratio from 0.6 to 0.9.

3.4 Pad Size Study

In this section, we change the pad diameters from 26μm to 39μm. It reveals that the maximum von Mises stress increases with the pad diameter as shown in Fig. 12.

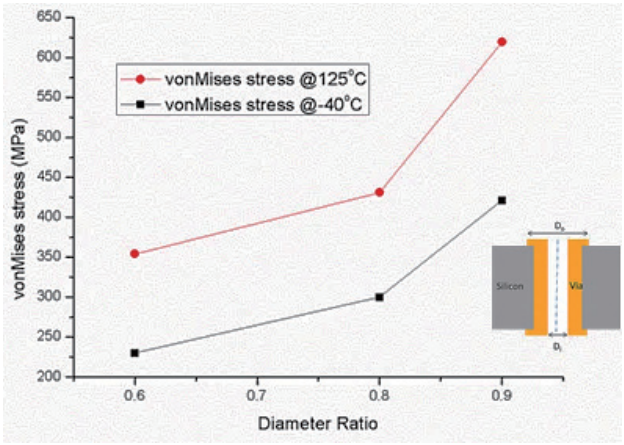


Fig. 11 Maximum von Mises stress at 125°C for the change of diameter ratio from 0.6 to 0.9.

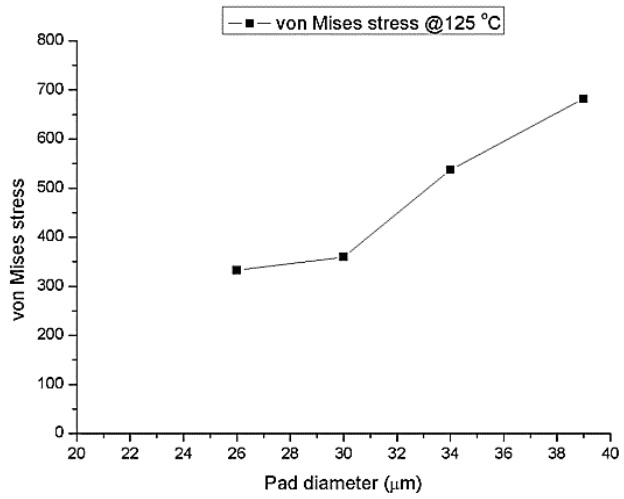


Fig. 12 Maximum von Mises stress at 125°C for pad diameter change from 26μm to 39μm.

https://doi.org/10.1017/jmech.2015.52 Published online by Cambridge University Press

3.5 TSV Pitch Study

Figure 13 shows the von Mises stress at TSV array center for the change of TSV pitch from 20μm to 50μm. The simulation result reveals that the von Mises stress at TSV array center decrease with the TSV pitch increase. This simulation result indicates that the TSV array pitch should be choose carefully between the stress-sensitive devices and TSV array.

3.6 Design of Experiments and Analysis of Variance

3.6.1 Maximum von Mises stress

In this study, design of experiments (DOE) and analysis of variance (ANOVA) are applied to determine which geometric parameter of TSV can lower the thermal stress most. DOE arranges the design factors of experiments and measures responses in an attempt to determine an effect. Four parameters are investigated at two levels, diameter ratio of TSV, pitch of TSV array, die thickness and pad diameter. In this study, full factorial design is constructed as shown in Table III. Table IV and Fig. 14 are the ANOVA result and half normal plot of maximum principal stress, respectively. The result reveals that the most significant factor is the pad diameter (D). The order of effect parameter is pad diameter (D), diameter ratio (A), pitch (C), interaction factor CD, and AD. As pad diameter and diameter ratio increase, the stress decrease as shown in Table V.

3.6.2 von Mises stress

Table 6 and Fig. 15 are the ANOVA result and half normal plot of von Mises stress, respectively. It reveals that the most significant factor in von Mises stress is also the pad diameter (D). The order of effect parameter is pad diameter (D), diameter ratio (A), pitch (C), interaction factor AD, and CD. Table 7 shows that the stress decreases as pad diameter and diameter ratio increase. The result is the same as the result of the maximum principal stress.

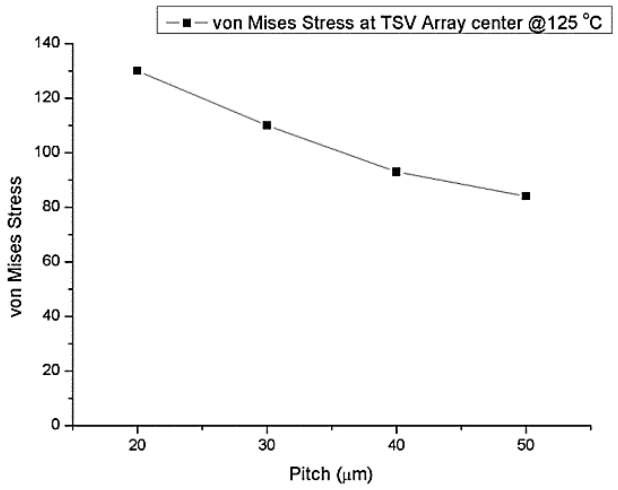


Fig. 13 von Mises stress at TSV array center for the change of TSV pitch from 20μm to 50μm.

Table 3 Full factorial design.

Factor	Diameter Ratio (A)	Die Thickness (B) (μm)	Pitch (C) (μm)	Pad Diameter (D) (μm)
Run				
1	0.6	75	20	39
2	0.8	50	30	39
3	0.8	50	30	30
4	0.8	75	30	39
5	0.6	50	20	39
6	0.8	75	30	30
7	0.8	50	20	30
8	0.6	50	30	39
9	0.6	50	20	30
10	0.8	50	20	39
11	0.6	50	30	30
12	0.6	75	20	30
13	0.6	75	30	39
14	0.8	75	20	30
15	0.6	75	30	30
16	0.8	75	20	39

Table 4 Anova result of maximum principal stress.

Source	Sum of Squares	Degree of Freedom	Mean Square	F Value
Model	3.90E+05	4	97486.69	24.22
A	41310.56	1	41310.56	10.26
C	5.56E+04	1	5.56E+04	13.81
D	2.53E+05	1	2.53E+05	62.79

Table 5 Coefficient estimate and standard error of maximum principal stress.

Factor	Coefficient Estimate	DF	Standard Error	95% CI Low	95% CI High	VIF
Intercept	450.44	1	15.86	415.53	485.35	
A-Diameter Ratio	50.81	1	15.86	15.90	85.72	1
C-Pitch	–58.94	1	15.86	–93.85	–24.03	1
D-Pad Diameter	125.69	1	15.86	90.78	160.60	1
CD	–50.19	1	15.86	–85.10	–15.28	1

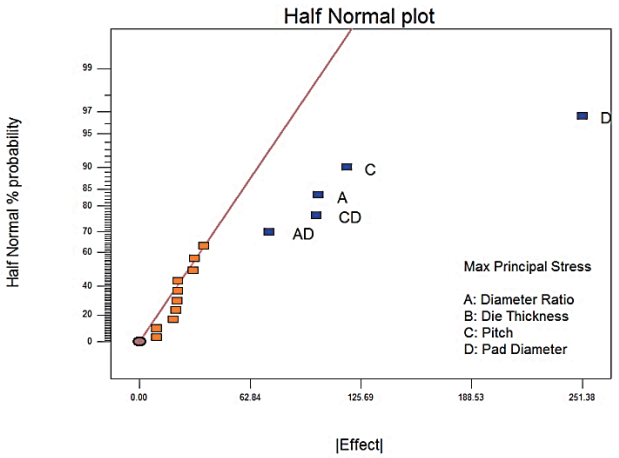


Fig. 14 Half normal plot of maximum principal stress.

https://doi.org/10.1017/jmech.2015.52 Published online by Cambridge University Press

Table 6 Anova result of von Mises stress.

Source	Sum of Squares	Degree of Freedom	Mean Square	F Value
Model	779250.75	5.00	155850.15	132.83
A	111556.00	1.00	111556.00	95.08
C	85556.25	1.00	85556.25	72.92
D	485112.25	1.00	485112.25	413.46
AD	49284.00	1.00	49284.00	42.00

Table 7 Coefficient estimate and standard error of von Mises stress.

Factor	Coefficient Estimate	DF	Standard Error	95% CI Low	95% CI High	VIF
Intercept	542.38	1	8.56	523.29	561.46	
A-Diameter Ratio	83.50	1	8.56	64.42	102.58	1
C-Pitch	–73.13	1	8.56	–92.21	–54.04	1
D-Pad Diameter	174.13	1	8.56	155.04	193.21	1
AD	55.50	1	8.56	36.42	74.58	1

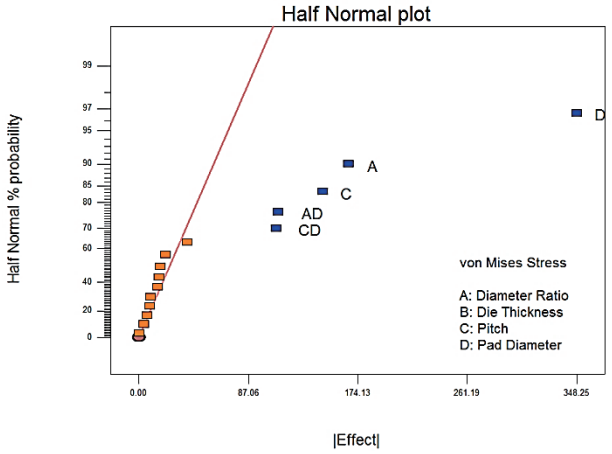


Fig. 15 Half normal plot of von Mises stress.

4. CONCLUSIONS

In this study, the thermal stress of TSV array and bonding under the accelerated thermal cycling are simulated. Due to the thermal expansion of TSV, the tensile stress occurs in the TSV structure. The stress analysis shows that the maximum thermal stress occurs not only at the nickel annular edge but also at the corners of pads. This may result in failure or delamination of TSV pads. Besides, the geometric parameters of TSV including diameter ratio and pad diameter effect are discussed by DOE and ANOVA. The maximum von Mises stress increases with diameter ratio and pad diameter. Based on these results, this study helps to obtain a clear thermal stress distribution of TSV array and possible failure regions in the TSV structure are obtained.

ACKNOWLEDGEMENTS

The authors would like to acknowledge the financial support from the National Ministry of Science and Technology of Taiwan under the contract numbers of MOST-103-3011-P-007-004 and MOST-101-2221-E-007-070-MY3.

REFERENCES

1. Beyne, E., "The rise of the 3rd dimension for system integration," *International Interconnect Technology Conference*, U.S.A. (2006).
2. McCracken, M. J., Koda, Y., Kim, H. J., Mayer, M., Persic, J., Hwang, J. S. and Moon, J.-T., "Explaining Nondestructive Bond Stress Data From High-Temperature Testing of Au-Al Wire Bonds," *IEEE Transactions on Components, Packaging, and Manufacturing Technology*, **3**, pp. 2029–2036 (2013).
3. Sayyad, A. S. and Ghugal, Y. M., "Effect of Stress Concentration on Laminated Plates," *Journal of Mechanics*, **29**, pp. 241–252 (2013).
4. Selvanayagam, C. S., Lau, J. H., Xiaowu Zhang, Seah, S. K. W., Vaidyanathan, K. and Chai, T. C., "Nonlinear Thermal Stress/Strain Analyses of Copper Filled TSV (Through Silicon Via) and Their Flip-Chip Microbumps," *IEEE Transactions on Advanced Packaging*., **32**, pp. 720–728 (2009).
5. Ryu. S. K., Jiang, T. F., Im, J., Ho, P. S. and Huang, R., "Thermomechanical Failure Analysis of Through-Silicon Via Interface Using a Shear-Lag Model with Cohesive Zone," *IEEE Transactions on Device and Materials Reliability*., **14**, pp. 318–326 (2014).
6. Koseski, R. P., Osborn, W. A., Stranick, S. J., DelRio, F. W., Vaudin, M. D., Dao, T., Adams, V. H. and Cook, R. F., "Micro-Scale Measurement and Modeling of Stress in Silicon Surrounding a Tungsten-Filled Through-Silicon Via," *Journal of Applied Physics.*, **110**, pp. 073517–073517-10 (2011).
7. Zhang, C. and Li, L., "Characterization and Design of Through-Silicon Via Arrays in Three-Dimensional Ics Based on Thermomechanical Modeling," *IEEE Transactions on Electron Devices*, **58**, pp. 279–287 (2011).
8. Ranganathan, N., Prasad, K., Balasubramanian, N. and Pey, K. L., "A Study of Thermo-Mechanical Stress and its Impact on Through-Silicon Vias," *IEEE Transactions on Electron Devices*, **18**, pp. 1–13 (2008).
9. Chen, Z. H., Song, X. H. and Liu, S., "Thermo-Mechanical Characterization of Copper Filled and Polymer Filled TSVs Considering Nonlinear Material Behaviors," *IEEE Transactions on Electron Devices*, U.S.A. (2009).
10. Liu, X., Chen, Q., Dixit, P., Chatterjee, R., Tummala, R. R. and Sitaraman, S. K., "Failure Mechanisms and Optimum Design for Electroplated Copper

https://doi.org/10.1017/jmech.2015.52 Published online by Cambridge University Press

Through-Silicon Vias (TSV)," *Electronic Components and Technology Conference*, U.S.A. (2009).
11. Lu, K. H., Ryu, S.-K., Zhao, Q., Zhang, X., Im, J., Huang, R. and Ho, P. S., "Thermal Stress Induced Delamination of Through Silicon Vias in 3-D Interconnects," *Proc. 60th ECTC*, Las Vegas, NV, U.S.A. (2010).
12. Athikulwongse, K., Chakraborty, A., Yang, J.-S., Pan, D. Z. and Lim, S. K., "Stress-Driven 3D-IC Placement with TSV Keep-Out Zone and Regularity Study," *IEEE/ACM ICCAD*, U.S.A. (2010).
13. Ladani, L. J., "Numerical Analysis of Thermo-Mechanical Reliability of Through Silicon Vias (TSVs) and Solder Interconnects in 3-Dimensional Integrated Circuits," *Microelectronic Engineering*, **87**, pp. 208–215 (2010).
14. Che, F. X., Lim, S. P. S., Chai, T. C. and Zhang, X., "Structure Design Optimization and Reliability Analysis on a Pyramidal-Shape Three-Die-Stacked Package with Through-Silicon Via," *IEEE Transactions on Device and Materials Reliability*, **12**, pp. 201–208 (2012).
15. Dudek, R., Bramer, B., Irsigler, R., Rzepke, S. and Michel, B., "Thermo-Mechanical Reliability Assessment for 3D Through-Si Stacking," *10th International Conference on Thermal, Mechanical and Multi-Physics Simulation and Experiments in Microelectronics and Microsystems*, Netherlands (2009).
16. MatWeb, *Material Property Data*, http://www.matweb.com (1996-2013).

(Manuscript received December 21, 2014, accepted for publication January 21, 2015.)

https://doi.org/10.1017/jmech.2015.52 Published online by Cambridge University Press